Dynamic Stereochemistry of Tetra-o-tolylcyclopentadienone

Rudolph Willem,* Henri Pepermans, Cornelis Hoogzand, Klaas Hallenga, and Marcel Gielen

Contribution from the Vrije Universiteit Brussel, AOSC-TW, Pleinlaan 2, B-1050 Brussels, Belgium. *Received August 28, 1980*

Abstract: The static and dynamic stereochemistry of tetra-*o*-tolylcyclopentadienone was examined theoretically by topological approaches. The temperature dependence of 100- and 270-MHz ^1H NMR and 67.89-MHz ^{13}C NMR spectra was also studied. The NMR spectra reveal two coalescence regions, below and above room temperature, ascribed to two different modes of rearrangement. The experimental results can be interpreted in terms of a tetracyclone skeleton having C_{2v} symmetry with the four aryl rings perpendicular to the plane of the cyclopentadienone. The low-temperature coalescence is most likely due to an uncorrelated one-ring rotation of an α-aryl ring while the high-temperature coalescence is due to an uncorrelated one-ring rotation of a β ring.

Introduction

Extensive research has been performed on the static and dynamic stereochemistry of organic molecules containing rotating aryl rings.[1,2] Mislow and co-workers have shown that systems such as triarylmethanes, triarylboranes, triarylamines, tetraarylmethanes, and 1,1,2,2-tetraarylethanes[1] exhibit a propeller-like structure. They undergo *correlated* flippings of the aryl rings, which means that the internal movement of one aryl ring is sensed by the other ones.[1u] In strong contrast to this, experimental data on hexa- and pentaarylbenzenes suggest that these molecules exist as structures in which the peripheral aryl rings are approximately perpendicular to the plane of the central ring.[2] Moreover, a detailed dynamic NMR study of some hexaarylbenzene derivatives led to the suggestion that these molecules undergo *uncorrelated* rotation of aryl rings; i.e., transition states involving more than one ring in the plane of the central benzene ring are energetically unfavorable. On the other hand, some ortho-substituted tetraarylporphyrin bases and their diprotonated derivatives also exhibit uncorrelated rotation of the aryl ring through the plane of the porphyrin macrocycle.[3]

Recently tetra-*o*-tolylcyclopentadienone was prepared by an organometallic reaction from di-*o*-tolylacetylene.[4] The synthesis and a discussion on the chemistry of tetra-*o*-tolylcyclopentadienone (TOTC) will be published elsewhere.[4] In this paper, we present the results of a detailed study on its stereochemical behavior and compare them with those obtained by Gust for hexaarylbenzenes.

On the Molecular Structure of Tetraarylcyclopentadienones

Besides a short communication[6] on 3,4-di-*o*-tolyl-2,5-diphenylcyclopentadienone which reveals interconversion between the cis and trans isomers with an activation barrier of approximately 23 kcal/mol, little is known about the static and the dynamic stereochemistry of tetraarylcyclopentadienones. While it is well established that hexaphenylbenzene exhibits a propeller conformation with torsional angles of ca. 65° in the solid state[2a,7] and a conformation with the peripheral rings perpendicular to the central ring, with oscillations of about 10° in the gas phase,[2a,8] similar data are not available for tetraphenylcyclopentadienone (=tetracyclone = TPC). There are some data[5,7-9] on TPC and substituted analogues that suggest that the conjugation of the carbonyl group with the β rings is very weak and virtually absent with the α rings; none of the phenyl rings of TPC lies in the plane of the five-membered ring and possibly the α rings lie somewhat more out of plane than the β ones. From the NMR spectra of TPC, studied by Arison[9a,b] and described in ref 5 together with two disubstituted tetracyclones, it was suggested that the four rings are steeply inclined with respect to that of the dienone system.[9a,b] We believe, in addition, that Arison's data indicate either a perpendicular position or a rapid internal rotation of the aryl rings. The ^{13}C NMR spectra[10] of TPC are not in contradiction with this idea.

It was shown by different techniques that tetraarylcyclone ketyl radicals[12] in solution and tetraarylcyclopentadienes or -pentenones[11] in the solid state do not exhibit identical skeleton structures,

(1) (a) J. D. Andose and K. Mislow, *J. Am. Chem. Soc.*, **96**, 2168 (1974); (b) J. F. Blount and K. Mislow, *Tetrahedron Lett.*, 909 (1975); (c) J. F. Blount, P. Finocchiaro, D. Gust, and K. Mislow, *J. Am. Chem. Soc.*, **95**, 7019 (1973); (d) R. J. Boettcher, D. Gust, and K. Mislow, *ibid.*, **95**, 7157 (1973); (e) D. A. Dougherty, K. Mislow, J. F. Blount, J. B. Wooten, and J. Jacobus, *ibid.*, **99**, 6149 (1977); (f) P. Finocchiaro, D. Gust, and K. Mislow, *ibid.*, **95**, 7029 (1973); (g) *ibid.*, **95**, 8172 (1973); (h) *ibid.*, **96**, 2165 (1974); (i) *ibid.*, **96**, 2176 (1974); (j) *ibid.*, **96**, 3198 (1974); (k) *ibid.*, **96**, 3205 (1974); (l) P. Finocchiaro, D. Gust, W. D. Hounshell, J. P. Hummel, P. Maravigna, and K. Mislow, *ibid.*, **98**, 4945 (1976); (m) P. Finocchiaro, W. D. Hounshell, and K. Mislow, *ibid.*, **98**, 4952 (1976); (n) D. Gust and K. Mislow, *ibid.*, **95**, 1535 (1973); (o) D. Gust, P. Finocchiaro, and K. Mislow, *Proc. Natl. Acad. Sci. U.S.A.*, **70**, 3445 (1973); (p) J. P. Hummel, D. Gust, and K. Mislow, *J. Am. Chem. Soc.*, **96**, 3679 (1974); (q) M. G. Hutchings, J. D. Andose, and K. Mislow, *ibid.*, **97**, 4553 (1975); (r) *ibid.*, **97**, 4562 (1975); (s) M. G. Hutchings, C. A. Maryanoff, and K. Mislow, *ibid.*, **95**, 7158 (1973); (t) M. R. Kates, J. D. Andose, P. Finocchiaro, D. Gust, and K. Mislow, *ibid.*, **97**, 1772 (1975); (u) K. Mislow, *Acc. Chem. Res.*, **9**, 26 (1976); (v) K. Mislow, D. Gust, P. Finocchiaro, and R. J. Boettcher, *Top. Curr. Chem.*, **47**, 1 (1974); (w) J. G. Nourse and K. Mislow, *J. Am. Chem. Soc.*, **97**, 4571 (1975); (x) K. S. Hayes, M. Nagumo, J. F. Blount, and K. Mislow, *ibid.*, **102**, 2773 (1980); (y) R. Glaser, J. F. Blount, and K. Mislow, *ibid.*, **102**, 2777 (1980); see also R. Willem and C. Hoogzand, *Org. Magn. Reson.*, **12**, 55 (1979); M. J. Sabacky, S. M. Johnson, J. C. Martin, and I. C. Paul, *J. Am. Chem. Soc.*, **91**, 7542 (1969).

(2) (a) D. Gust, *J. Am. Chem. Soc.*, **99**, 6980 (1977); (b) D. Gust and A. Patton, *ibid.*, **100**, 8175 (1978); (c) A. Patton, J. Wang Dirks, and D. Gust, *J. Org. Chem.*, **44**, 4749 (1979).

(3) J. Wang Dirks, G. Underwood, J. C. Matheson, and D. Gust, *J. Org. Chem.*, **44**, 2551 (1979), and references cited therein.

(4) C. Hoogzand, H. Pepermans, and R. Willem, submitted for publication.

(5) M. A. Ogliaruso, M. G. Romanelli, and E. I. Becker, *Chem. Rev.*, **65**, 261 (1965), and references cited therein.

(6) J. Haywood-Farmer and M. A. Battiste, *Chem. Ind. (London)*, 1232 (1971).

(7) (a) E. D. Bergmann and E. Fischer, *Bull. Soc. Chim. Fr.*, **17**, 1084, (1950); (b) H. Calus, *Rocz. Chem.*, **28**, 85 (1954); (c) A. Di Giacomo and C. P. Smyth, *J. Am. Chem. Soc.*, **74**, 4411 (1952).

(8) (a) C. F. H. Allen and R. Y. Ning, *Can. J. Chem.*, **42**, 2151 (1964); (b) E. D. Bergmann, G. Berthier, D. Ginsburg, Y. Hirshberg, D. Lavie, S. Pinchas, B. Pullmann, and A. Pullmann, *Bull. Soc. Chim. Fr.*, **18**, 661 (1951); (c) R. N. Jones, C. Sandorfy, and D. E. Trucker, *J. Phys. Radium*, **15**, 320 (1954), and references cited therein.

(9) (a) B. H. Arison, unpublished work cited in ref 4a; (b) *Diss. Abstr. B*, **28**, 1847 (1967); (c) S. B. Coan, D. E. Trucker, and E. I. Becker, *J. Am. Chem. Soc.*, **75**, 900 (1953); (d) *ibid.*, **77**, 60 (1955); (e) V. F. d'Agostino, M. J. Dunn, A. E. Ehrlich, and E. I. Becker, *J. Org. Chem.*, **23**, 1539 (1958); (f) M. Koral, *Diss. Abstr. B*, **17**, 1468 (1957); (g) E. L. Shapiro and E. I. Becker, *J. Am. Chem. Soc.*, **75**, 4769 (1953); (h) F. J. Thaller, D. E. Trucker, and E. I. Becker, *ibid.*, **73**, 228 (1951), and references cited therein.

(10) L. Knothe and H. Prinzbach, *Justus Liebigs Ann. Chem.*, 687 (1977).

0002-7863/81/1503-2297$01.25/0

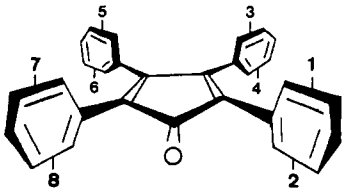

Figure 1. Representation of the C_{2v} ideal "perpendicular" structure of tetraphenylcyclopentadienone (TPC) with skeleton numbering.

but the aryl rings lie neither in the plane of nor perpendicular to the central five-membered ring. In contrast to this, an X-ray structure determination shows that in 2,5-di-*tert*-butyl-3-(4-chlorophenyl)cyclopentadienone[13] the aryl ring is nearly perpendicular to the central ring. It appears from the literature that no clear data are available which prove that tetraarylcylopentadienones have either a perpendicular or a propeller conformation. A fully planar structure can safely be excluded for steric reasons, as confirmed by spectroscopic data (see ref 7–9). Because the results of Gust and co-workers[2] on hexa- and pentaarylbenzenes lead to the most straightforward interpretations in terms of the skeleton structure in which the peripheral rings are perpendicular to the central ring, we confine the detailed argumentation to the skeleton in which the four aryl rings are perpendicular to the five-membered ring. Nevertheless, the propeller structure cannot be excluded unambiguously and a short qualitative part of the discussion of the results will be devoted to this point.

Static Stereochemistry of Tetra-*o*-tolylcyclopentadienone (TOTC) with a Perpendicular C_{2v} Skeleton Structure

If we assume the four aryl rings of TOTC to be perpendicular to the five-membered ring, the molecular *skeleton* of the idealized *TPC* has C_{2v} symmetry on the NMR time scale and can be represented as in Figure 1. In TOTC each phenyl ring bears a methyl group at one of the ortho positions. As a consequence the four aryl rings lose their local C_2 symmetry axis so that the symmetry of the whole molecule is lowered. If, in addition, the internal rotations about the four C_6–C_5 ring bonds, the only possible rearrangements in TOTC, are completely frozen out on NMR time scale, then rotational isomerism in TOTC becomes possible according to the number and relative positions of the methyl groups lying above or below the cyclopentadienone ring.[2]

The number of isomers can be calculated according to a group theoretical approach,[14-16] but this is somewhat tedious when the number of isomers is relatively small, as in this case. Therefore we prefer to use an approach similar to that proposed by Mislow[1u,15b] which is based on the "binary character" of the possible positions of a methyl group, above or below the C_5 ring. In the former situation the CH_3 group is represented by the symbol 1 and in the latter one by the symbol 0. Since there are four methyl groups, the total number of configurations[15c] is $2^4 = 16$, each of which is represented by what we propose to call a "*configuration matrix*". The upper row of such a 2×2 matrix represents the position of the β-methyl groups while the lower one represents that of the α-methyl groups. The example for Figure 2 visualizes this clearly.

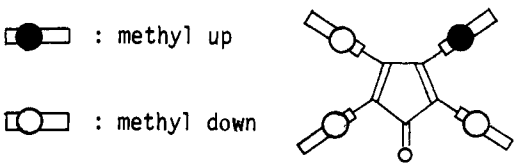

Configuration matrix :

$$\begin{pmatrix} 0 & 1 \\ 0 & 0 \end{pmatrix}$$

Figure 2. One of the sixteen possible configurations of TOTC and its corresponding configuration matrix.

Now the 16 configuration matrices which can be constructed in this way do not all correspond to different isomers of TOTC. Indeed due to the *o*-methyl group on each aryl ring, the plane of the central ring of the ideal C_{2v} structure of TPC is no longer a symmetry element of TOTC. Therefore the isomers of TOTC can keep as sole symmetry elements the C_2 axis, the plane perpendicular to the central ring, or none of them and can consequently only have as symmetry point group C_2, C_s or C_1, the only subgroups of C_{2v}.

If we apply now an operator r, representing a rotation of 180° about the C_2 axis, to any of the configuration matrices of TOTC, the matrix elements are changed in such a way that all the symbols of the left (right) column having value 1(0) appear, after application of the rotation, on the right (left) column with the value 0(1). An example makes this clear:

$$r\begin{pmatrix} 1 & 1 \\ 0 & 1 \end{pmatrix} = \begin{pmatrix} 0 & 0 \\ 0 & 1 \end{pmatrix}$$

Configurations having C_2 symmetry are characterized by a configuration matrix remaining invariant under the operator r; e.g.

$$r\begin{pmatrix} 1 & 0 \\ 1 & 0 \end{pmatrix} = \begin{pmatrix} 1 & 0 \\ 1 & 0 \end{pmatrix}$$

Since the application of a rotation operator such as r does not generate a new isomer, a pair of configuration matrices related by such an operator represents one isomer. Clearly, isomers having C_2 symmetry are characterized by only one configuration matrix while those having C_s or C_1 symmetry are characterized by two configuration matrices. This fact is an illustration of the mathematically proven theorem that the number of configurations of one isomer is proportional to the inverse of its symmetry number.[14,15d,16]

Application of a reflection operator s through the plane perpendicular to the central ring to the configuration matrices of TOTC merely exchanges the two columns of matrix; e.g.

$$s\begin{pmatrix} 1 & 1 \\ 0 & 1 \end{pmatrix} = \begin{pmatrix} 1 & 1 \\ 1 & 0 \end{pmatrix}$$

Configuration matrices having two identical columns remain invariant under s and represent achiral isomers with C_s symmetry. They are, however, represented by two configuration matrices (symmetry number 1); e.g.

$$s\begin{pmatrix} 0 & 0 \\ 1 & 1 \end{pmatrix} = \begin{pmatrix} 0 & 0 \\ 1 & 1 \end{pmatrix} \text{ in contrast to } r\begin{pmatrix} 0 & 0 \\ 1 & 1 \end{pmatrix} = \begin{pmatrix} 1 & 1 \\ 0 & 0 \end{pmatrix}$$

Configuration matrices remaining invariant under neither r nor s correspond to chiral isomers having C_1 symmetry. It should be noted that none of the configuration matrices can remain invariant under both r and s operators since none of the isomers of TOTC

(11) (a) G. Evrard, P. Piret, G. Germain, and M. Van Meersche, *Acta Crystallogr., Sect. B*, **27**, 661 (1971); (b) G. Evrard, P. Piret, and M. Van Meersche, *Bull. Soc. Chim. Belg.*, **80**, 159 (1971); (c) R. L. Harlow and S. H. Simonsen, *Cryst. Struct. Commun.*, **6**, 695 (1977).

(12) (a) W. Broser, H. Kurreck, D. Rennoch, and J. Reusch, *Tetrahedron*, **29**, 3959 (1973); (b) H. T. Grunder, H. J. Haink, H. Kurreck, W. J. Juergen, and W. D. Woggon, *Z. Naturforsch., B*, **27**, 532 (1972), and references cited therein; see also R. D. Allendoerfer and A. S. Pollack, *Mol. Phys.*, **22**, 661 (1971).

(13) A. Nishinaga, T. Itahara, T. Matsuura, A. Rieker, D. Koch, K. Albert, and P. Hitchcock, *J. Am. Chem. Soc.*, **100**, 1826 (1978).

(14) E. Ruch, W. Hässelbarth, and B. Richter, *Theor. Chim. Acta*, **19**, 288 (1970); see also Chapter 8 of ref 15a.

(15) (a) J. Brocas, M. Gielen, and R. Willem, "The Permutational Approach to Dynamic Stereochemistry", McGraw-Hill, New York, in press; (b) *ibid.*, Chapter 13, Section 13-1; (c) *ibid.*, Chapter 4, Sections 4-1 and 4-2, and Chapter 8, Section 8-1; (d) *ibid.*, Chapter 8, Sections 8-4 and 8-5; (e) *ibid*, Chapter 12, Section 12-5; (f) *ibid.*, Chapter 12, Sections 12-2 and 12-3; (g) *ibid.*, Chapter 4, Section 4-3; (h) *ibid.*, Section 4-4; (i) *ibid.*, Chapter 7, Sections 7-1, 7-2, and 7-3; (j) *ibid.*, Chapter 5, Section 5-6; (k) *ibid.*, Section 5-5; (l) *ibid.*, Chapter 9; (m) *ibid.*, Section 9-8; (n) *ibid.*, Chapter 12, Sections 12-5 and 12-6; (o) *ibid.*, Section 12-7.

(16) (a) R. Willem, Ph.D. Thesis, Université Libre de Bruxelles; (b) J. Brocas and R. Willem, *Bull. Soc. Chim. Belges*, **82**, 479 (1973); (c) D. J. Klein and A. H. Cowley, *J. Am. Chem. Soc.*, **97**, 1633 (1975); (d) *ibid.*, **100**, 2593 (1978).

Table I. Isomers, Configurations, and Predicted NMR Resonances in Fully Frozen Out TOTC

isomer numbering	configuration matrices	point group	numbering of magnetic sites: ^{13}CO	α-CH_3	β-CH_3
I_1	$\begin{pmatrix}0&0\\0&0\end{pmatrix}\xrightarrow{r}\begin{pmatrix}1&1\\1&1\end{pmatrix}$	C_s	1	1α	1β
I_2	$\begin{pmatrix}0&0\\1&0\end{pmatrix}\xrightarrow{r}\begin{pmatrix}1&1\\1&0\end{pmatrix}$				
	$\downarrow s$ $\quad$ $\downarrow s$	C_1	2	2α, 3α	2β, 3β
$I_{\bar{2}}$	$\begin{pmatrix}0&0\\0&1\end{pmatrix}\xrightarrow{r}\begin{pmatrix}1&1\\0&1\end{pmatrix}$				
I_3	$\begin{pmatrix}0&0\\1&1\end{pmatrix}\xrightarrow{r}\begin{pmatrix}1&1\\0&0\end{pmatrix}$	C_s	3	4α	4β
I_4	$\begin{pmatrix}1&0\\1&0\end{pmatrix}$				
	$\downarrow s$	C_2	4	5α	5β
$I_{\bar{4}}$	$\begin{pmatrix}0&1\\0&1\end{pmatrix}$				
I_5	$\begin{pmatrix}1&0\\0&0\end{pmatrix}\xrightarrow{r}\begin{pmatrix}1&0\\1&1\end{pmatrix}$				
	$\downarrow s$ $\quad$ $\downarrow s$	C_1	5	6α, 7α	6β, 7β
$I_{\bar{5}}$	$\begin{pmatrix}0&1\\0&0\end{pmatrix}\xrightarrow{r}\begin{pmatrix}0&1\\1&1\end{pmatrix}$				
I_6	$\begin{pmatrix}1&0\\0&1\end{pmatrix}$				
	$\downarrow s$	C_2	6	8α	8β
$I_{\bar{6}}$	$\begin{pmatrix}0&1\\1&0\end{pmatrix}$				
total no. of predicted resonances			6	8	8

can have C_{2v} symmetry, as mentioned above.

Using these operators, one can easily generate and count all of the possible isomers from the 16 possible configuration matrices. The 10 possible rotational isomers of TOTC are set up in Table I, together with their configurations, point group, and the NMR characteristics necessary for the NMR spectral analysis. It appears from Table I that the 10 isomers are subdivided into two achiral isomers of C_s symmetry, I_1 and I_3, two pairs of enantiomers of C_2 symmetry, I_4,$I_{\bar{4}}$ and I_6,$I_{\bar{6}}$, and two pairs of enantiomers of C_1 symmetry, I_2,$I_{\bar{2}}$ and I_5,$I_{\bar{5}}$.

Since NMR spectra of enantiomers are identical in achiral environment[17] and each isomer bears only one carbonyl group, it is easy to predict that when rotational isomerizations are completely frozen out, the ^{13}C NMR spectrum should exhibit six carbonyl signals, each of them being representative of one of the six diastereoisomers I_j (j = 1, 3) or diastereomeric pairs of enantiomers I_k, $I_{\bar{k}}$ (k = 2, 4, 5, 6). These carbonyl resonances are numbered according to the corresponding isomer or pair of enantiomers. The number of methyl signals is somewhat less trivially predicted.

First of all, it is worthwhile to note that the methyl groups of the α and β rings are heterotopic[17] since the α and β rings are constitutionally different. Since the number of α- and β-CH_3 groups is the same in each isomer, the total number of NMR α-CH_3 signals accordingly must be equal to the total number of β-CH_3 ones.

The C_2 pairs of enantiomers, I_4,$I_{\bar{4}}$ and I_6,$I_{\bar{6}}$, must give rise to *one* α-CH_3 signal each since the α-CH_3 groups within each isomer are *homotopic*.[15e,17]

The achiral C_s isomers, I_1 and I_3, should also give rise to *one* α-CH_3 signal each, in an achiral medium, since the α-CH_3 groups within each isomer are *enantiotopic*.[15e,17]

Finally the C_1 pairs of enantiomers, I_2,$I_{\bar{2}}$ and I_5,$I_{\bar{5}}$, must give rise to *two* α-CH_3 signals each since here the α-CH_3 groups within each isomer are *diastereotopic*.[15e,17] Similar arguments hold for the β-CH_3 signals. Therefore 8 α-CH_3 signals and 8 β-CH_3 signals, together 16, are to be expected in TOTC when the isomerizations are frozen out. They are numbered as in Table I.

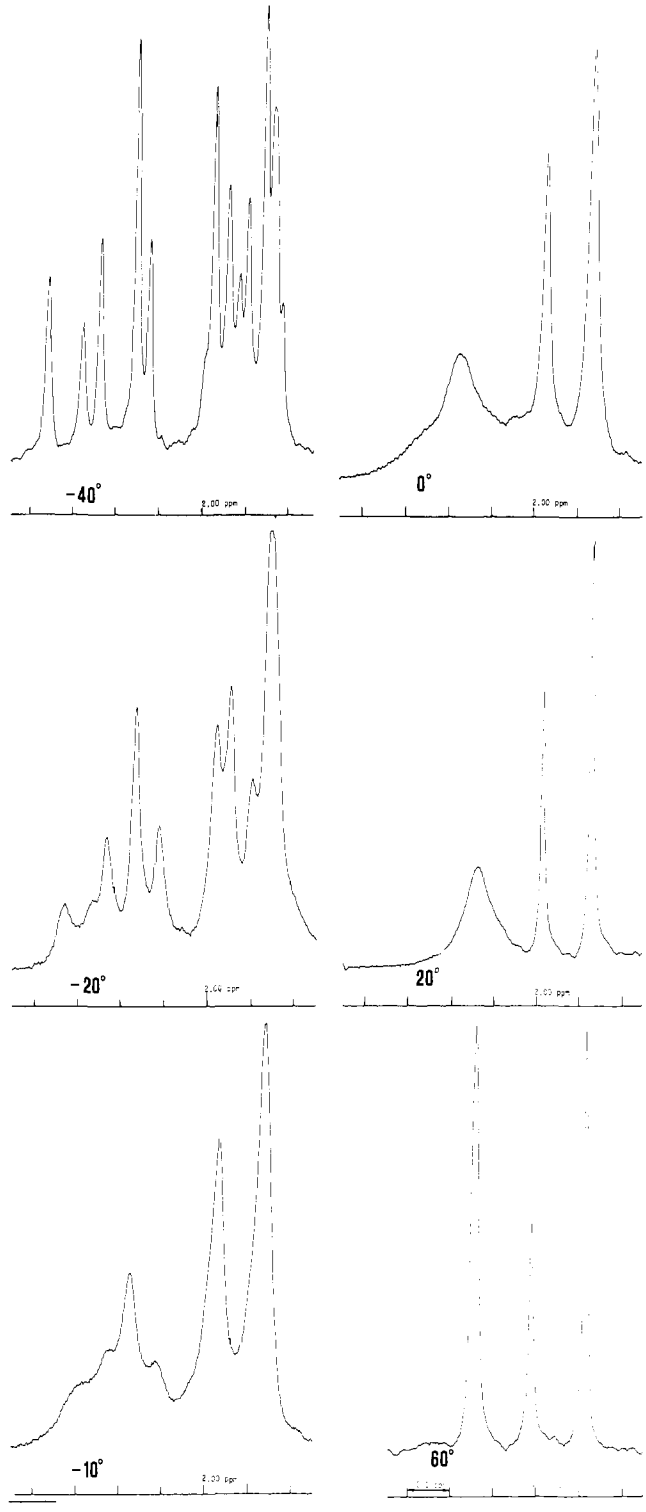

Figure 3. Temperature-dependent 270-MHz ^1H NMR FT spectra (methyl region) of TOTC in $CDCl_3$.

Experimental Low-Temperature NMR Spectra. Probable Static Skeleton Structure of TOTC

The 270-MHz ^1H NMR FT spectrum of TOTC in $CDCl_3$, in the methyl region, at −40 °C (see Figure 3) exhibits 12 more or less well-defined signals. Below this temperature, the spectra (not shown here) exhibit a similar behavior with more accidental isochronies, the value of the chemical shifts showing a strong temperature dependence. When the enhancement method of Ernst[18] is used, the signals are narrowed and a better resolution

(17) (a) M. Raban and K. Mislow, *Top. Stereochem.* **1**, 1 (1967); (b) K. Mislow, "Introduction to Stereochemistry", W. A. Benjamin, New York, 1966; (c) J. Reisse, R. Ottinger, P. Bickart, and K. Mislow, *J. Am. Chem. Soc.*, **100**, 911 (1978); (d) K. Mislow, *Bull. Soc. Chim. Belg.*, **86**, 595 (1977).

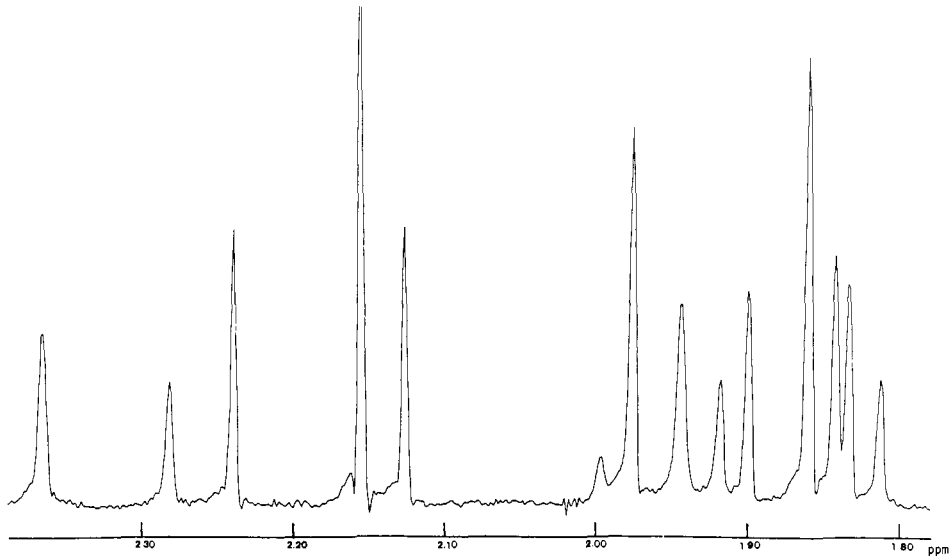

Figure 4. 270-MHz ^1H NMR FT spectrum of TOTC in $CDCl_3$ at −40 °C using the enhancement method of Ernst (see Experimental Section and ref 18). The fourth peak from the left is off scale.

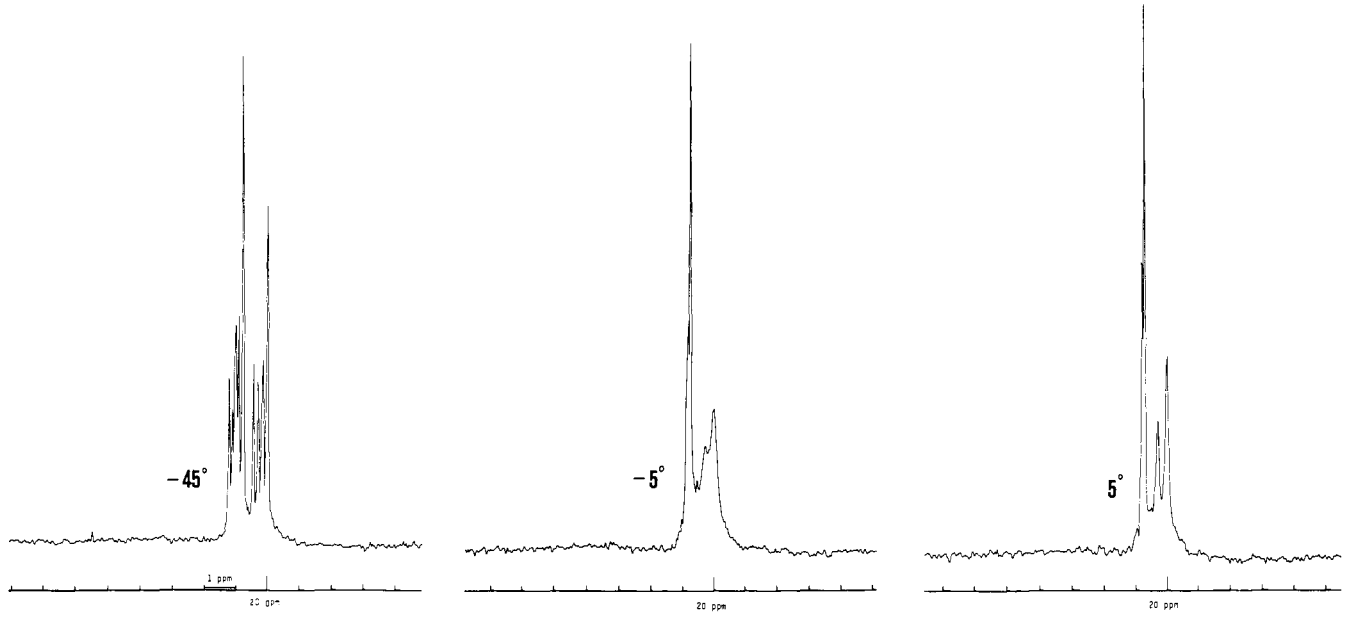

Figure 5. Temperature-dependent ^{13}C NMR FT spectra at 67.89 MHz of TOTC in $CDCl_3$ (methyl region).

is obtained. Figure 4 shows such an enhanced 270-MHz ^1H NMR FT spectrum of TOTC in $CDCl_3$ at −40 °C, in the methyl region; it exhibits at least 13 and perhaps 14 signals if the smallest peak is taken into account. The small distortion of each signal is not due to an improper phasing but is caused by a slight overenhancement.

The 67.89-MHz ^{13}C NMR spectrum of TOTC in $CDCl_3$, in the methyl region, at −45 °C, exhibits nine well-defined signals (see Figure 5). A similar behavior is observed up to −30 °C and at −50 °C with more signal overlapping. Finally, its 67.89-MHz ^{13}C NMR spectrum in $CDCl_3$, in the carbonyl region, at −50 °C exhibits five more or less well-defined signals (see Figure 6).

The number of experimentally observed signals is always smaller than the number of predicted signals, namely 16 methyl and 6 carbonyl lines. This means that the observed spectra are compatible with the C_{2v} skeleton structure proposed for TOTC. That the number of observed signals is smaller than the number of predicted ones can be attributed to one or both of the following possibilities.

1. Accidental Isochronies. This phenomenon is especially encountered when a large number of resonances arises in a small frequency range, as in this case. Moreover, it is clear from Figures 3, 5, 6, and 7 that various coalescence phenomena occur. If now some pair of signals is characterized by an intrinsic chemical shift difference that is much smaller than the chemical shift difference between the signals of another pair, then the former may have already coalesced at the lowest temperature available, even if the latter coalesce only at higher temperatures, as far, of course, as these coalescences are due to the same dynamic process or, at least, to processes with rate constants having similar values and temperature dependences.[15f,19] In this respect, one should note that the frequency range (~100 Hz) of the methyl signals in the ^{13}C spectra is smaller than that (~160 Hz) of the methyl signals in

(18) (a) R. R. Ernst, *Adv. Magn. Reson.*, **2**, 1 (1968); (b) A. G. Ferrige and J. C. Lindon, *J. Magn. Reson.*, **31**, 337 (1978).

(19) See, e.g., (a) J. A. Pople, W. G. Schneider, and H. J. Bernstein, "High Resolution Nuclear Magnetic Resonance", McGraw-Hill, New York, 1959, Chapter 10; (b) J. W. Emsley, J. Feeney, and L. H. Sutcliffe, "High Resolution Nuclear Magnetic Resonance Spectroscopy", Pergamon Press, New York, 1968, Chapter 9; (c) H. S. Gutowsky and C. H. Holm, *J. Chem. Phys.*, **25**, 1228 (1956); (d) H. Shanan-Atidi and K. H. Bar-Eli, *J. Phys. Chem.*, **74**, 961 (1970); (e) H. S. Gutowsky, J. Jonas, and T. H. Siddall III, *J. Am. Chem. Soc.*, **89**, 4300 (1967).

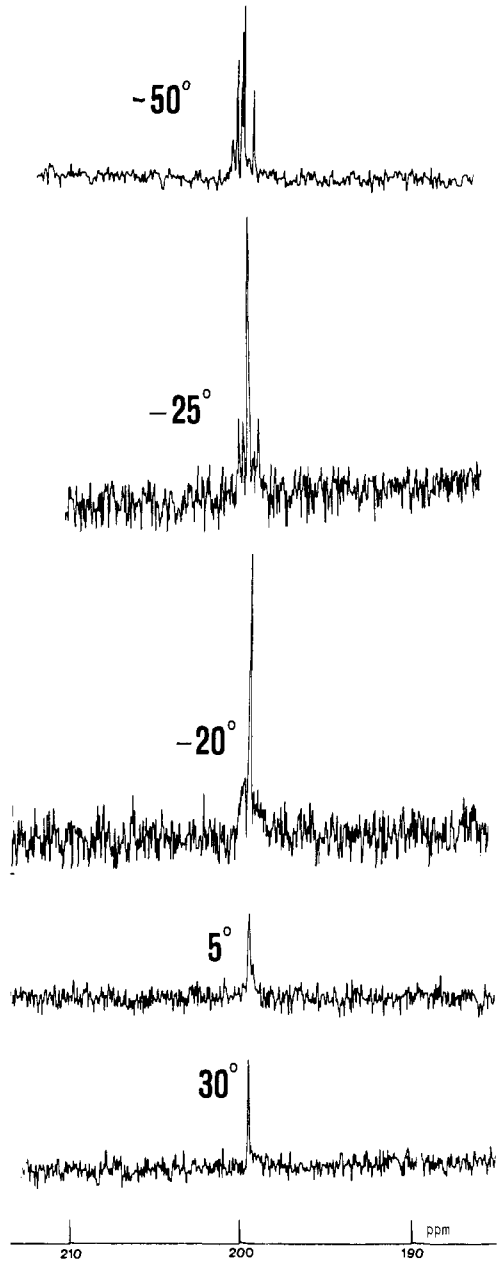

Figure 6. Temperature-dependent ^{13}C NMR FT spectra at 67.89 MHz of TOTC in $CDCl_3$ (carbonyl region; see Experimental Section).

the ^1H spectra, so that it is not really surprising to observe fewer methyl signals for ^{13}C than for ^1H at low temperature.

2. One Isomer Is Much Less Abundant Than the Other Ones. This possibility arises from the fact that in none of the ^{13}C spectra in the carbonyl region between −50 and −30 °C six rather than five well-defined signals are observed. At most, in the spectrum at −50 °C it is possible to note six peaks although the sixth is hardly more intense than the noise. If one of the diastereoisomers or diastereomeric pairs is less abundant, its associated carbonyl signal may disappear in the noise. This idea is compatible with the presence of the small peak in the spectrum of Figure 4, although the latter could also be due to an impurity.

Nevertheless, why should it not be possible that the isomer with the four methyl groups on the same side of the cyclopentadienone ring is more sterically hindered, and hence less abundant, than the other ones?

Dynamic Stereochemistry of TPC. Theoretical Description

The coalescences of Figures 3, 5, 6, and 7 show that the internal rotations of the *o*-tolyl groups relating the isomers of TOTC become rapid on the NMR time scale. In order to get a precise description of these rearrangements for TOTC, one needs to gain,

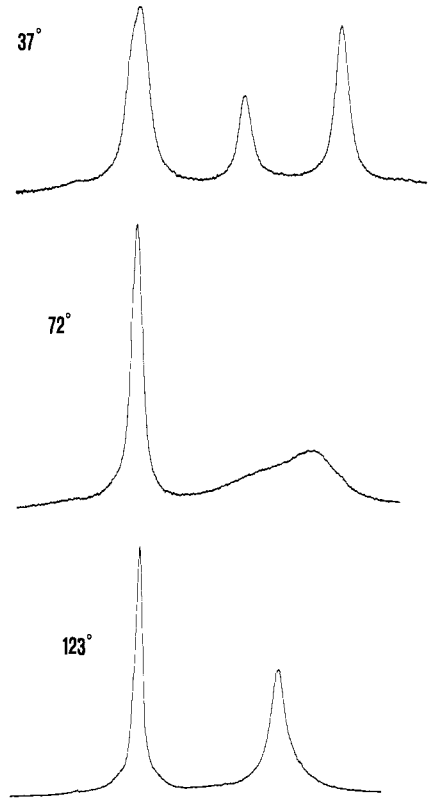

Figure 7. Temperature-dependent ^1H NMR CW spectra at 100 MHz of TOTC in *o*-dichlorobenzene (methyl region).

first of all, precise insight into the rearrangements of the idealized molecular skeleton from which TOTC is derived. We assume that this idealized skeleton is the C_{2v} one represented in Figure 1. The group theoretical permutation approach[2,15,16a,c,d,20] is particularly appropriate to find *all* the possible sets of rearrangements, the *modes of rearrangement*, of a given molecular skeleton. A mode of rearrangement[2,15h,16a,c,d,20] is a set of elementary pathways which are indistinguishable because either they are characterized by the same initial and final configuration states, they occur with the same rate constant because they are symmetry equivalent,[15h,16a] or they are related to each other by a combination of both equivalence relations. Using now the skeleton numbering given in Figure 1, we see that the permutation (12),[21] e.g., gives a representation of an internal rotation in which the edges 1 and 2 of the corresponding α-phenyl ring are permuted. This representation is not unique since the permutation (1827)(36)(45)[21] represents an internal rotation of the *same* ring preceded by an overall rotation of 180° of the whole molecule about the C_2 axis. The permutation (78) represents now the internal rotation of the *other* α-phenyl ring. Hence (12) and (78) represent different kinetic pathways (they lead to different configurations[15c]), which, however, proceed with the same rate since they represent *symmetry equivalent* internal rotations. Moreover, (1728)(36)(45) represents the same internal rotation as (78), preceded by an overall rotation of the molecule. The permutations {(12),(78),(1827)(36)-

(20) (a) M. Gielen and N. van Lautem, *Bull. Soc. Chim. Belg.*, **79**, 679 (1970); (b) W. G. Klemperer, *J. Chem. Phys.*, **56**, 5478 (1972); (c) *Inorg. Chem.*, **11**, 2668 (1972); (d) *J. Am. Chem. Soc.*, **94**, 6940 (1972); (e) *ibid.*, **94**, 8360 (1972); (f) *ibid.*, **95**, 380 (1973); (g) *ibid.*, **95**, 2105 (1973); (h) in "Dynamic Nuclear Magnetic Resonance Spectroscopy", L. M. Jackman and F. A. Cotton, Eds., Academic Press, New York, 1975, Chapter 2; (i) M. G. Hutchings, J. B. Johnson, W. G. Klemperer, and R. R. Knight, *J. Am. Chem. Soc.*, **99**, 7126 (1977); (j) J. I. Musher, *Inorg. Chem.*, **11**, 2335 (1972); (k) *J. Am. Chem. Soc.*, **94**, 5662 (1972); (l) W. Hässelbarth and E. Ruch, *Theor. Chim. Acta*, **29**, 259 (1973); (m) J. G. Nourse, *J. Am. Chem. Soc.*, **99**, 2063 (1977); (n) R. Willem, *J. Chem. Soc., Dalton Trans.*, 33 (1979).

(21) (1827)(36)(45) means edge 1 is replaced by edge 8, edge 8 is replaced by edge 2, edge 2 is replaced by edge 7, edge 7 is replaced by edge 1; edge 3 is replaced by edge 6 and conversely; edge 4 is replaced by edge 5 and conversely.

Table II. Modes of Rearrangement of TPC and Their Characteristics

mode	permutations		type	connectivity	transition state(s)
M_0	I = (1)(2)(3)(4)(5)(6)(7)(8) (18)(27)(36)(45)		identity (overall skeleton rotation)	1	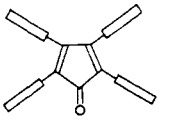
M_1	(78) (1728)(36)(45)	(12) (1827)(36)(45)	α-one-ring rotation	2	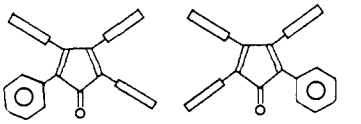
M_2	(56) (18)(27)(3546)	(34) (18)(27)(3645)	β-one-ring rotation	2	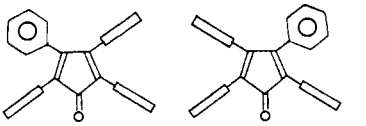
M_3	(12)(78) (17)(28)(36)(45)		αα-two-ring rotation	1	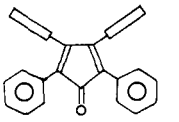
M_4	(56)(78) (1728)(3546)	(12)(34) (1827)(3645)	αβ-cis-two-ring rotation	2	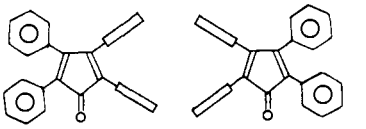
M_5	(12)(56) (1827)(3546)	(34)(78) (1728)(3645)	αβ-trans-two-ring rotation	2	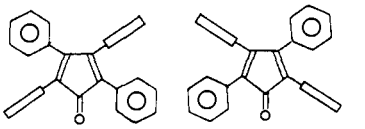
M_6	(34)(56) (18)(27)(35)(46)		ββ-two-ring rotation	1	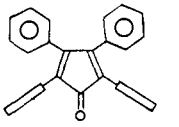
M_7	(12)(56)(78) (17)(28)(3546)	(12)(34)(78) (17)(28)(3645)	ααβ-three-ring rotation	2	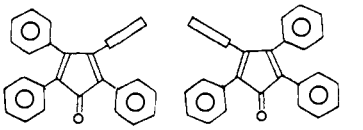
M_8	(34)(56)(78) (1728)(35)(46)	(12)(34)(56) (1827)(35)(46)	ββα-three-ring rotation	2	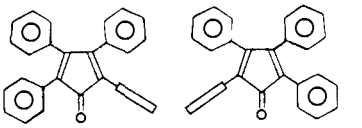
M_9	(12)(34)(56)(78) (17)(28)(35)(46)		four-ring rotation (reflection)	1	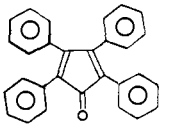

(45),(1728)(36)(45)} are said to constitute the same mode of rearrangement since they represent indistinguishable pathways. This mode can be called the α-one-ring rotation and has connectivity[15h,22] 2 since it can proceed in two different but symmetry-equivalent ways.

All of the modes of TPC, generated either mathematically using a double coset approach[15,16,20,23] or simply by inspection as in the above example, are set up in Table II. With each mode are given the permutations constituting it, the type of internal rotation it corresponds to, its connectivity, and the associated transition state(s) (see ref 2b for a comparison with the modes of hexaphenylbenzene). Four modes of connectivity 1, M_0, M_3, M_6, and M_9, are characterized by a transition state having a C_{2v} symmetry while the six other ones of connectivity 2, M_1, M_2, M_4, M_5, M_7, and M_8, are characterized by a C_s transition state.

Dynamic Stereochemistry of TOTC. Theoretical Description

To set up the isomerization scheme of all the isomers of TOTC under each mode of TPC, we apply the modes of TPC (Table II) to each isomer of TOTC. This quite straightforward approach hides, however, some pitfalls because the symmetry of the isomers of TOTC is *lower* than that of TPC, the idealized C_{2v} skeleton. The problem is namely that all the arrangements of a given mode

(22) (a) E. L. Muetterties, *J. Am. Chem. Soc.*, **91**, 1636 (1969); (b) *ibid.*, **91**, 4115 (1969).

(23) The group of allowed permutations $S = \{S_2^{12} \otimes S_2^{34} \otimes S_2^{56} \otimes S_2^{78}\}$ Λ A has to be partitioned in unions of double cosets of the type $A \times A \cup A\sigma \times \sigma^{-1}A$, where $A = C_2 = \{I,(18)(27)(36)(45)\}$ is the rotational symmetry group of TPC and σ is an improper symmetry operation of TPC, for instance, (17)(28)(35)(46). For more details on the mathematical approach, see ref 15i–l, 16c,d, and 20. A discussion on the concept of the group of allowed permutations is given in ref 20b–f and is reviewed in ref 15i.

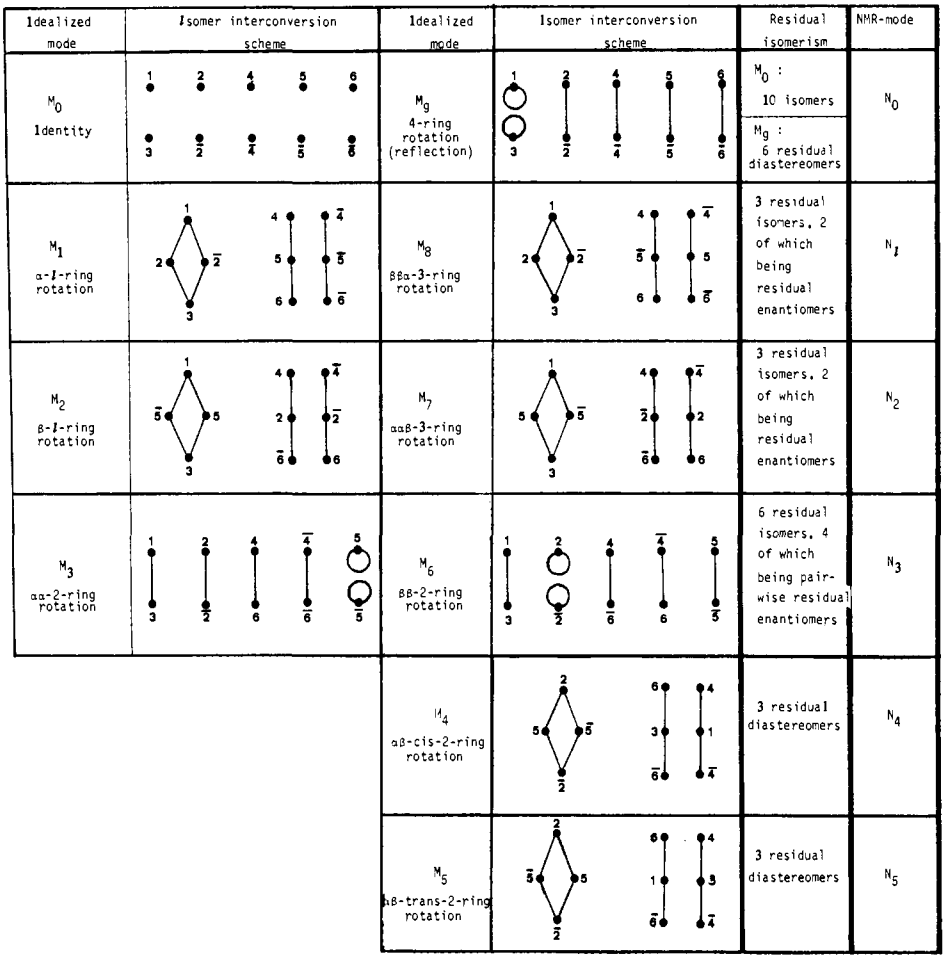

Figure 8. Interconversion schemes of all the isomers under each idealized mode of rearrangement and NMR modes to which they belong.

proceed with different rate constants since they are applied to isomers having *different* energies. A priori it is not impossible that rearrangements of a mode of TPC applied to different isomers of TOTC have very different rate constants and, on the other hand, that a mode M_x applied to isomer A proceeds with a rate similar to that of a mode M_y applied to isomer B. In these cases the concept of modes, applicable to TPC, *cannot* be extended to less symmetric systems such as TOTC, and each rearrangement between a pair of isomers constitutes a mode by itself. Therefore, if we want to interpret the NMR results of TOTC in terms of modes of the ideal skeleton, i.e., in terms of *idealized* modes,[15m,24] we have to make a fundamental assumption which has often been made by Mislow[1] and Gust[2] in the interpretation of experimental NMR results, namely, the assumption of *noninterdigitation*[1m] of idealized modes.[15m,24] Hereby it is assumed that *one* rearrangement of an idealized mode applied to *different* isomers or *different* rearrangements within an idealized mode applied to the *same* isomer proceed with rate constants of the same order of magnitude, while rearrangements of another idealized mode proceed with rate constants of a different order of magnitude; the physical meaning[1m,24] of this assumption is that the *skeletons* of the initial state and of the transition state determine the order of magnitude of the rate constants while the substituents act as perturbations and modify more or less this order of magnitude. The idealized mode corresponding to the set of highest rate constants (lowest activation energies) is called the threshold mode.[1]

When one of the nontrivial modes of connectivity 1 (M_3, M_6, M_9) is applied to one of the ten possible isomers of TOTC, one of these isomers is generated. This can simply be done by changing, in (one of) the configuration matrix(ces) of that isomer, the digit(s) that corresponds (correspond) to the ring(s) undergoing internal rotation.[1]

The result of the application of an idealized mode of connectivity 2 (M_1, M_2, M_4, M_5, M_7, M_8) to an isomer depends on the symmetry of that isomer. If the starting isomer of TOTC is of symmetry C_2 or C_s, the two kinetic pathways of modes with connectivity 2 remain symmetry equivalent and lead, respectively, to the same final isomer or to enantiomers. These pathways proceed therefore with the same rate constant. If, however, the starting isomer is of symmetry C_1, the two kinetic pathways of such modes are no longer symmetry equivalent. They lead to different isomers and proceed therefore with different rate constants. For example

$$M_i \begin{pmatrix} 1 & 0 \\ 0 & 0 \end{pmatrix} \begin{cases} \nearrow \begin{pmatrix} 1 & 0 \\ 0 & 1 \end{pmatrix} & I_6\ (C_2) \\ \searrow \begin{pmatrix} 1 & 0 \\ 1 & 0 \end{pmatrix} & I_4\ (C_2) \end{cases} \text{diastereoisomers}$$

$I_5\ (C_1)$

It should also be noted that while for TPC, each mode is characterized by only one internal rotation mechanism, for TOTC, each idealized mode can be characterized by different mechanisms. For instance, an α ring of TOTC can rotate with its methyl group adjacent either to the carbonyl group or to the neighboring β ring.[27]

(24) (a) J. Brocas, R. Willem, D. Fastenakel, and J. Buschen, *Bull. Soc. Chim. Belg.*, **84**, 483 (1975); (b) J. Brocas, R. Willem, J. Buschen, and D. Fastenakel, *ibid.*, **88**, 415 (1979); (c) R. Willem, J. Brocas, and D. Fastenakel, *Theor. Chim. Acta*, **40**, 25 (1975); (d) R. Willem, J. Brocas, J. Buschen, and A. M. Decoster, *Mol. Phys.*, **35**, 349 (1978).

(25) (a) H. M. McConnell, *J. Chem. Phys.*, **28**, 430 (1958); (b) C. S. Johnson and C. G. Moreland, *J. Chem. Educ.*, **50**, 477 (1973); (c) H. S. Gutowsky, D. W. Mac Call, and C. P. Slichter, *J. Chem. Phys.*, **21**, 279 (1953); (d) H. S. Gutowsky and A. Saika, *ibid.*, **21**, 1688 (1953); (e) H. S. Gutowsky and C. J. Hoffman, *Phys. Rev.*, **80**, 110 (1950), and references cited therein.

(26) For a review, see K. Mislow, D. A. Dougherty, and W. D. Hounshell, *Bull. Soc. Chim. Belg.*, **87**, 555 (**1978**), and references cited therein.

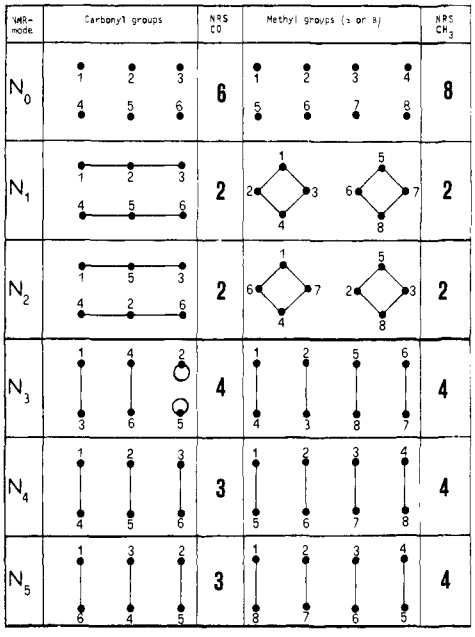

Figure 9. Magnetic site interconversion schemes under each NMR mode of TOTC. The schemes given in the right column are equally valid for the α- and β-methyl groups. NRS = number of residual signals.

When each idealized mode of TPC is applied to all of the isomers of TOTC, a complete scheme of the interconversion of the isomers under each mode is obtained. These schemes are conveniently represented by graphs. They are represented in Figure 8, in which the isomer numbering of Table I has been used.

A set of isomers connected to each other by a given idealized mode is called a residual isomer.[1j,m,u] For instance, it appears from Figure 8 that sets of isomers $\{1,2,3,\bar{2}\}$ and $\{4,5,6\}$ and the sets $\{4,5,6\}$ and $\{\bar{4},\bar{5},\bar{6}\}$ are, respectively residual diastereoisomers and enantiomers under M_1. Of course, the concept of residual isomer can only be defined in connection with a given idealized mode of rearrangement becoming rapid on the observational time scale.[1j,m,u] Clearly, there are four types of nontrivial idealized modes of TOTC, according to the number of residual isomers to which they give rise: M_9, six residual diastereoisomers; M_3 and M_6, six residual isomers, four of which are pairwise residual enantiomers; M_4 and M_5, three residual diastereoisomers; M_1, M_2, M_7, and M_8, three residual isomers, two of which are residual enantiomers. This is, of course, an interesting criterion of distinguishability of idealized modes in dynamic NMR experiments. Now, some of the idealized modes which are a priori distinguishable become indistinguishable because of the fundamental inability of NMR spectroscopy to distinguish enantiomers or enantiotopic sites in an achiral environment. It is, for instance, clear that the a priori distinguishable interconversion schemes 4-5-6 and 4-$\bar{5}$-6 of M_1 and M_8, respectively, become therefore indistinguishable. A set of modes of rearrangement which are indistinguishable because the kinetic analysis is performed by NMR in an achiral environment is called an *NMR mode*.[15n,16c,20g,24c,d] In Figure 8, idealized modes of rearrangement belonging to the same NMR mode appear on the same row. That, for instance, M_1 and M_8 belong to the same NMR mode N_1 can also be felt intuitively by noting that an α-one-ring rotation leads to the same magnetic site exchange as a $\beta\beta\alpha$-three-ring rotation combined to a reflection, which is unobservable by NMR in achiral solvents. Using the interconversion schemes of isomers under each idealized mode, one can find the magnetic site transfer schemes associated with each NMR mode. Again, these magnetic site transfer schemes can be represented conveniently by graphs. They are given in Figure 9 for the carbonyl sites and for the magnetic sites associated with the methyl groups, the graphs being identical for the α- and β-methyl groups. The magnetic site numbering used is that given in Table I. Since, in the experimental conditions used here, enantiotopic sites are indistinguishable, they are characterized by the same labeling (see Table I).

It is seen that each scheme is characterized by a variable number of subgraphs. Each subgraph represents a set of signals that coalesce when the mode responsible for that interconversion becomes rapid on the NMR time scale. It also represents the remaining signal when coalescence is achieved in the rapid-exchange region. Such a signal is said to be a residual signal, and when for a given NMR mode more than one residual signal is observed, that NMR mode is said to exhibit residual diastereotopism.[1k,m,n]

Figure 9 shows that since it is not possible to attribute each signal of the spectra to the isomer from which it arises, it is impossible to distinguish the NMR modes N_1 and N_2 because they are characterized, in the ^{13}CO spectrum as well as in the methyl spectrum, by the same number of residual signals. A similar argument holds for N_4 and N_5. The NMR mode N_3 is, in principle, distinguishable from N_4 and N_5 since their respective numbers of residual lines in the ^{13}CO spectrum are expected to be different (four vs. three) although the number of residual methyl signals is the same. Before starting a comparison of the expected coalescence behaviors for the distinguishable NMR modes with the experimentally observed ones, we emphasize that the results of Figure 9 describe a situation in which no accidental isochrony of residual lines arises.

Experimental Coalescence Behavior and Residual Diastereotopism. Probable Modes of Rearrangement in TOTC

The temperature-dependent 270-MHz FT ^1H NMR spectra (in the methyl region) of TOTC in $CDCl_3$ exhibit a complex coalescence behavior (Figure 3). Between −40 and −10 °C the resonance lines of the upfield part of the spectrum coalesce into two residual signals of unequal intensity (coalescence I). In the same temperature range the low-field signals undergo some broadening. Between −20 and +20 °C the low-field resonances coalesce to one very broad line (coalescence II). At 60 °C the spectrum exhibits three residual signals, a broad low-field one and two narrower high-field ones with approximate intensity ratio 5:2:3. This behavior is confirmed by the 100-MHz CW ^1H NMR spectrum of TOTC in *o*-dichlorobenzene at 37 °C (Figure 7) although the low-field resonance exhibits a small low-field shoulder. This shoulder is much more apparent in the 270-MHz FT ^1H NMR spectrum in *o*-$C_6H_4Cl_2$ at 30 °C, not shown in this paper. Finally the 67.89-MHz ^{13}C NMR spectrum in $CDCl_3$ at 5 °C (Figure 5), in the methyl region, clearly exhibits *four* residual resonances, the two low-field ones being very close together. This shows that the low-field residual signal of the methyl 270- and 100-MHz ^1H NMR spectra above 0 °C is, in fact, a superposition of two accidentally isochronous residual signals. The 100-MHz CW ^1H NMR spectra (Figure 7) in *o*-$C_6H_4Cl_2$ show that the two residual high-field resonances coalesce at 72 °C (coalescence III) and give rise to one single line while the low-field resonance further narrows as the temperature increases, so that the spectrum at 123 °C exhibits two equally intense residual signals, one being due to the methyl group of the α-tolyl groups of TOTC and the other to those of the β ones, the interconversions between all the isomers being rapid on the NMR time scale. We attribute the low-field resonance to the α-methyl group and the high-field one to the β-methyl group. Indeed the latter results from the coalescence of two unequally intense lines appearing at 1.99 and 1.88 ppm at 30 °C in $CDCl_3$, chemical shifts which are very close to those observed (2.04 and 1.90 ppm at 37 °C in the same solvent) for the two unequally intense methyl resonances of 3,4-di-*o*-tolyl-2,5-diphenylcyclopentadienone[6] while the α signal of TOTC has a quite different chemical shift, 2.14 ppm at 30 °C.

No further attempt was made to confirm this attribution since it is not essential for our analysis of the dynamic stereochemistry of TOTC. We understand these coalescences and residual spectra as follows. We attribute coalescences I and II to the same set of dynamic processes, the low-temperature set of processes, the low-field coalescence II representing the α-CH_3 groups and the

(27) We thank one of the referees for bringing our attention to this point.

Table III. Combinations of Modes That Can Explain the Presence of Only One Residual Line in the High-Temperature ^1H NMR Spectrum

threshold mode	possible high-temperature modes
M_1	M_2, M_7, M_4, M_5
M_2	M_1, M_8, M_4, M_5
M_7	M_1, M_8, M_4, M_5
M_8	M_2, M_7, M_4, M_5

high-field coalescence I representing the β-CH_3 groups. These coalescences lead to two pairs of residual signals as shown by the ^{13}C spectrum (Figure 5), the two α-residual signals being accidentally isochronous in the ^1H spectrum (Figures 3 and 7). That coalescences I and II are observed at different temperatures is readily explained by the fact that the coalescing lines are much more spread out in frequency in the low-field region (ca. 120 Hz) than in the high-field region (maximum 50 Hz). Therefore, the low-field resonances coalesce at a higher value of the rate constant, and hence of temperature, than the high-field ones. We attribute coalescence III of the two high-field residual lines at higher temperature to another set of processes, called heretoafter the high-temperature set of processes. That the coalescence of the two low-field residual lines under these high-temperature processes cannot be observed in the ^1H spectrum is evident because of their isochrony; moreover, even if they were slightly anisochronous at other temperatures, the much smaller chemical shift difference of the low-field residual resonances, compared to that of the high-field residual ones, cause the former ones to coalesce at lower temperature than the latter ones. The presence of two α- and two β-residual lines can readily be explained in terms of two residual diastereomers, which is only compatible (see Figure 9) with the NMR modes N_1 and N_2 becoming rapid on the NMR time scale. Therefore, we exclude the idealized modes of the NMR modes N_3, N_4, and N_5 as being responsible for the low-temperature coalescences I and II. The only idealized modes that can explain these low-temperature processes are M_1, M_2, M_7, and M_8, as appears from Figure 8.

The existence of two residual diastereoisomers is not clearly confirmed by the ^{13}C carbonyl spectra (see Figure 6), although a small high-field shoulder near the most intense peak is observed at 5 °C; moreover, the spectrum at −20 °C exhibits a broad line almost disappearing in the noise, together with a very narrow line resulting possibly from the accidentally isochronous and/or coalescing resonances that appear very close together in the spectra at −50 and −40 °C, which is perhaps also an indication for the presence of the two residual diastereoisomers. The ^{13}C methyl spectrum at +5 °C (Figure 5) and even higher temperatures leaves fortunately no doubt about that question.

If the threshold idealized mode of rearrangement responsible for coalescences I and II is indeed one of the modes M_1, M_2, M_7, or M_8, the high-temperature set of processes must be due to another idealized mode, that combined with one of the possible threshold modes can explain coalescence III (Figure 7) and the unique residual signal in the carbonyl spectrum at and above 30 °C (Figure 6). To find out which modes can do so, we look in Figure 9 at the NMR modes which interconvert magnetic sites that are not interconverted by N_1 or N_2 alone. It is indeed sufficient to find the NMR modes that interconvert any two magnetic sites belonging to different subgraphs of the exchange patterns of N_1 or N_2 to explain the coalescence due to the high-temperature set of processes. If N_1 is taken as threshold NMR mode, then the combinations $N_1 + N_2$, $N_1 + N_4$, and $N_1 + N_5$ can explain coalescence III, while if N_2 is taken as the threshold NMR mode, the combinations $N_2 + N_1$, $N_2 + N_4$, and $N_2 + N_5$ do so. Combinations of N_1 or N_2 with N_3 or N_0 are clearly excluded. This leads to the sixteen possible combinations of idealized modes of rearrangement given in Table III.

So far, we have reached the limit of the information that can be extracted from the NMR data for TOTC. A further choice of the combination of idealized modes that is responsible for the coalescences observed must be made from qualitative energetic considerations.

Most Likely Internal Rotation Mechanism of TOTC

Among the four possible threshold modes, M_1, M_2, M_7, or M_8, we note that the former two are characterized by transition states with only one ring lying in the plane of the cyclopentadienone ring, while the latter two both have three rings in that plane (see Table II). It is quite evident that the latter situation leads to much more steric congestion than the former, so we exclude M_7 or M_8 as threshold modes. Hence, the only possible combinations which remain are those of the two first rows of Table III.

Comparing the combinations $M_1 + M_2$ with $M_1 + M_7$ and $M_2 + M_1$ with $M_2 + M_8$, we note that we must exclude the combinations $M_1 + M_7$ and $M_2 + M_8$ for the same reasons which led us to exclude M_7 and M_8 as threshold modes. On the other hand, we consider the idealized mode M_5 to be of only academic interest since we do not find any electronic or steric argument that could explain why nonneighboring α and β rings should rotate at the same time. Finally, since the transition states of the idealized mode M_4 involve two neighboring rings in the plane of the central ring while M_1 and M_2 involve only one ring in that plane, we are naturally led to prefer $M_1 + M_2$ and $M_2 + M_1$ to $M_1 + M_4$ and $M_2 + M_4$, respectively. Hence the only alternative is the choice between $M_1 + M_2$ and $M_2 + M_1$. Gust and co-workers pointed out in their study[2b,c] of the dynamic stereochemistry of pentaarylbenzenes of the type XC_6Ar_5 that the rings adjacent to the X substituent rotate much more rapidly than the other rings if the substituent X is less bulky than an aryl ring.

A similar situation arises in TOTC, where the carbonyl group is certainly less sterically demanding than an aryl ring. Therefore, we suggest that in TOTC the α rings rotate faster than the β ones because the α rings are surrounded by only one aryl ring while the β rings are surrounded by two such rings. Hence we adopt the combination of modes $M_1 + M_2$ as being the most realistic explanation of the dynamic NMR results of TOTC. The model with the α-one-ring rotation as the threshold idealized mode and the β-one-ring rotation as the idealized mode with a higher steric hindrance is not only a remarkable example of chemical simplicity but also receives some additional qualitative support from comparison with results obtained for other systems, which is discussed in the next section.

Comparison with Other Systems

The best model system to which TOTC can be compared is 3,4-di-*o*-tolyl-2,5-diphenylcyclopentadienone (**1**) for which some data are available.[6] We have already mentioned that at room temperature the NMR spectrum exhibits two unequally intense β-methyl signals than can be ascribed to the cis and the trans isomers of **1**, having as a skeleton structure the C_{2v} one proposed for TPC and TOTC. At 133 °C these two methyl signals coalesce to one signal,[6] indicating that internal rotations of the β-*o*-tolyl rings become rapid on the NMR time scale, while the rotation of the α-phenyl rings have, of course, no influence on the β-methyl NMR spectrum throughout the whole temperature range. Of all the idealized modes listed in Table II only M_2, M_4, M_5, and M_7 can induce cis–trans isomerization in **1**.

The next step is, of course, to compare the activation parameters of the rearrangements of TOTC and **1**. A precise determination of the activation parameters of the threshold mode is impossible because of the complexity of the spectra, the impossibility of attributing each line to its respective isomer, and a fortiori of determining the relative population of the isomers; there are also a great number of processes that are responsible for these coalescences. We believe the activation parameters for these processes to fluctuate by a few kcal/mol about the value of 15 kcal/mol. A determination of the activation parameters of the high-temperature set of processes by a full line-shape analysis based on the formalism of Bloch–Mac Call,[15a,19,25] using an approach similar to that of Gutowsky and co-workers,[19e] gave very poor correlations in an Eyring least-squares analysis. We attribute this to the fact that no correlation between the chemical shift difference and the temperature could be found, both because the temperature range of which we dispose between the two coalescence regions is too small and because this dependence is probably very complicated

because it depends on the individual properties of all the isomers. For the same reason, the temperature dependence of the equilibrium ratio (about 0.4/0.6) of the two residual diastereoisomers appeared to be of the order of magnitude of the experimental error on its determination so that here again no good Van't Hoff–Le Châtelier correlations could be obtained. Also, the choice of the natural line width is subject to errors because it has to be done *between* the coalescences so that the values choosen contain certainly nonnegligible contributions due to the chemical exchange.

Furthermore, the simulations shoud be based on an isomer interconversion pattern resulting from the modes $M_1 + M_2$. In this pattern a great number of rate constants are involved and since the line-shape analysis has to be performed on residual lines, a stepwise approach similar to that used by Gust and explained in the experimental section of his paper[2b] is impossible here. Therefore we prefer to limit ourselves to a rough estimation of the free enthalpy of activation for the interconversion of the two residual isomers, using a graphical method described in the literature.[19d] Using the chemical shift difference of 13 Hz found in the spectrum of Figure 7 at 37 °C and the population ratio of the residual diastereomers A and B of 0.4 vs. 0.6, assumed to be temperature independent, we find $(\Delta G^{\ddagger}_{345})_{A\rightarrow B} = 19.7$ kcal/mol and $(\Delta G^{\ddagger}_{345})_{B\rightarrow A} = 20.0$ kcal/mol. The activation energy given[6] for **1** is 23 ± 3 kcal/mol compares reasonably well with our estimation of 20 kcal/mol for the high-temperature set of processes of TOTC.

If we now assume that this means that the high-temperature set of processes in TOTC and the rearrangement in **1** are due to the same idealized mode of rearrangement, we may safely exclude M_1 as the idealized mode for the high-temperature processes of TOTC since M_1 cannot lead to any coalescence in **1**. A similar argument holds for M_8 so that on this basis the combinations $M_2 + M_1$, $M_2 + M_8$, $M_7 + M_1$, and $M_7 + M_8$ may be safely excluded for TOTC. We feel this gives additional support for favoring $M_1 + M_2$ over $M_2 + M_1$.

On this basis, it is even possible to propose a *mechanism* for the threshold mode M_1; a priori, the rotation of an α ring can proceed with the methyl group directed toward either the carbonyl group or the neighboring β ring. If the latter situation is occurring, it would be expected that the α-ring rotation should proceed with an activation energy similar to that of the β-ring rotation, since in these cases the activation parameters are essentially determined by the interaction between the methyl group and the neighboring aryl ring. Since it is observed that the α-ring rotation proceeds with a substantially lower activation energy than the β-ring rotation, we deduce that the α ring rotates with its methyl group directed toward the carbonyl group.[27]

Last, but not least, none of the results obtained by Gust[2] is in contradiction with the proposal that aryl rings in hexa- and pentaarylbenzenes rotate uncorrelated through one-ring rotations. We arrive independently at a similar conclusion for TOTC, so this type of internal rotation mechanism seems to be quite general for molecules containing peripheral rings attached to a central ring.

We point out that the model proposed above is not the only possible explanation for the experimental results. We did not look at models explaining our results without the assumption of noninterdigitation of modes although they possibly exist (we believe them to be unlikely). We did, however, check our results in light of a propeller-like skeleton structure of C_2 symmetry. If the isomers of TOTC are completely frozen out in a propeller-like structure, the NMR spectra in the carbonyl and in the methyl region should exhibit, respectively, 10 and 32 resonances instead of 6 and 16 for the C_{2v} structure. This is never observed, even at −60 °C. Nevertheless, a detailed analysis of the idealized modes of rearrangement of TOTC, assuming the C_2 propeller-like skeleton, reveals that exactly the same combinations of modes as for the C_{2v} structure explain equally well the experimental coalescence behaviors, provided the propeller inverts its configuration rapidly on the NMR time scale even at −60 °C through a concerted four-ring flip with the C_{2v} skeleton as transition state. It is indeed easy to convince oneself that the isomers of the propeller skeleton interconvert pairwise under the four-ring flip to give residual isomers, the averaged symmetry and structure of which are in one-to-one correspondence with those of the isomers of TOTC in the C_{2v} structure so that these two situations are NMR indistinguishable.

The only somewhat formal question that can still be asked is that of whether the C_{2v} structure results from the averaging of a rapidly proceeding four-ring flip in the propeller structure, corresponding therefore to a low-lying potential maximum between the two potential minima of the right- and left-handed propeller structures, or, to the contrary, whether the C_{2v} structure corresponds to a potential minimum about which the four aryl rings oscillate concerted with a more or less large amplitude, as is the case for hexaphenylbenzene in the gas phase.[2a,8] This interesting problem can be approached by force field calculations[26] but not by dynamic NMR.

Experimental Section

Characteristics of TOTC. The synthesis of TOTC will be described elsewhere.[4] It is a brick red powder with a melting point of 146–147 °C. Anal. Calcd. for $C_{33}H_{28}O$: C, 89.95; H, 6.42. Found: C, 89.95; H, 6.20. IR (KBr) 1700 cm^{-1} (carbonylstretch); UV (ethanol) λ_{max} 213 (ϵ 54 000 M^{-1} cm^{-1}), 250 (17 500), 337 (6500), 458 nm (770); MS base peak at *m/e* 440; ^1H NMR ($CDCl_3$, 270 MHz, Me_4Si, −40 °C) 6.68–7.15 (H_{ar}), 1.82, 1.84, 1.86, 1.90, 1.92, 1.95, 1.98, 2.12, 2.15, 2.24, 2.28, and 2.36 (CH_3) ppm; ^1H NMR ($CDCl_3$, 270 MHz, Me_4Si 20 °C) 1.88, 1.99, 2.14 (broad band) (CH_3) ppm; ^{13}C NMR ($CDCl_3$, 67.89 MHz, room temperature, Me_4Si internal standard) 20–22 (CH_3), 125–138 (C_{ar}), 133 (α-C), 157 (β-C), 200 (C=O) ppm (compares fairly well with the ^{13}C characteristics of tetraphenylcyclopentadienone:[10] 127–133 (C_{ar}), 125 (α-C), 155 (β-C), 200 (C=O)); ^1H NMR (*o*-dichlorobenzene, 100 MHz, HMS internal standard) 37 °C, 1.82, 1.95, 2.08 ppm (intensity ratios 1:0.4:0.6); 72 °C, 1.87, 2.10 ppm; 123 °C, 1.92, 2.10 ppm (intensity ratio 1:1).

Instruments. High-resolution 270-MHz ^1H NMR spectra were obtained on a Bruker HX270 spectrometer. It was equipped with an Aspect 2000 computer and a B-VT 1000 temperature controller with a low-temperature attachment. The ^{13}C spectra at 67.89 MHz were measured on the Bruker HX270, using 4-W ^1H broad-band decoupling power. The resolution of the ^1H spectra at 270 MHz has been enhanced by using the Lorentz–Gauss (L/G) line transformation.[18] The assumed Lorentz line widths were 4 Hz; the Gaussian line widths obtained were 2.3 Hz.

The same enhancement routine has also been used in the ^{13}C spectra to improve the signal-to-noise ratio (S/N) of the CO signals. As has been shown by Ernst[18a] for the optimum filter, the S/N improvement obtained by application of the L/G transformation is far superior to the S/N improvement possible with the standard exponential filter at the same loss in resolution. The Lorentz line width assumed for the CO's was 6 Hz; the obtained Gaussian line width was 5 Hz. The number of accumulations was 2000 for each of the ^{13}C experiments. The 100-MHz spectra at high temperatures were recorded on a JEOL MH100 spectrometer. The temperature determinations were based on the temperature dependence of the chemical shift difference between the alcohol and the 2-methylene protons of 1,3-propanediol.

IR spectra were recorded on a Perkin-Elmer 257, the UV–vis absorption spectrum on a Perkin-Elmer 402, and the mass spectrum on a AEI MS902S. The melting point was determined with a Reichert Thermopan microscope.

Acknowledgment. We are indebted to Professor Dr. J. Brocas and Professor Dr. J. Reisse for helpful discussions and to Mr. F. Resseler, Mr. Polain, and Mr. M. Desmet for recording, respectively, the 270-MHz, 100-MHz, and mass spectra. H.P. is an aspirant at the Belgian Nationaal Fonds voor Wetenschappelijk Onderzoek, the financial support of which is acknowledged. Assistance of Dr. E. Van Oost and Dr. Ir. G. Baron in writing computer programs is gratefully acknowledged. We thank Dr. M. De Blecker of the society Christiaens N.V. for performing the elemental analysis and Dr. B. De Poorter, Mr. I. Van den Eynde, and Mr. J. Van Biesen for their constructive remarks.